

Protein–Lipid Interactions in Zein Films Investigated by Surface Plasmon Resonance

QIN WANG,[†] ANTONY R. CROFTS,[§] AND GRACIELA W. PADUA^{*,†}

Department of Food Science and Human Nutrition, University of Illinois, 382/D AESB, 1304 West Pennsylvania Avenue, Urbana, Illinois 61801, and Department of Biochemistry, 419 Roger Adams Laboratory B-4, 600 South Mathews Avenue, University of Illinois, Urbana, Illinois 61801

Experiments on the adsorption of α -zein (characterized by SDS-PAGE) from aqueous ethanol and 2-propanol solutions onto hydrophilic and hydrophobic surfaces are reported. Zein adsorption onto self-assembled monolayers (SAMs) was detected by surface plasmon resonance (SPR). Gold substrates were prepared by thermal evaporation on glass slides. Gold-coated surfaces were modified by depositing SAMs of either a long-chain carboxylic acid terminated thiol [COOH(CH₂)₁₀SH] or a methyl-terminated alkanethiol [CH₃(CH₂)₇SH]. Experimental measurements indicated that zein interacted with both hydrophilic and hydrophobic surfaces. Zein concentration affected the thickness of bound zein layers. The estimated thickness of the zein monolayer deposited on hydrophilic surfaces was 4.7 nm. Zein monolayer thickness on hydrophobic surfaces was estimated at 4.6 nm. The topography of zein layers was examined by atomic force microscopy (AFM) after solvent was evaporated. Surface features of zein deposits depended on the adsorbing surface. On hydrophilic surfaces, roughness values were high and distinct ring-shaped structures were observed. On hydrophobic surfaces, zein formed a uniform and featureless coverage.

KEYWORDS: Zein; surface plasmon resonance; protein–fatty acid interaction; biodegradable plastics; atomic force microscopy

INTRODUCTION

Zein has been studied for its potential to produce free-standing edible/biodegradable films (1, 2). Films made exclusively from zein are rigid and very brittle. Therefore, one or more plasticizers are normally added in the film-making process. Commonly used plasticizers are liquid organic compounds such as polyols, mono-, di-, and oligosaccharides, lipids, and lipid derivatives (3). Fatty acids (i.e., palmitic acid, stearic acid, linolenic acid, and oleic acid) were used in the preparation of zein resins from which films were drawn (2, 4). Physical properties of zein–fatty acid films including tensile properties, water resistance, and gas permeability were affected by film structure and protein–lipid interactions (4, 5).

Zein conformation in alcohol solutions was investigated by circular dichroism (6) and X-ray scattering measurements (7). Both studies considered that the spatial–structure model for zein contains 9 or 10 successive helical segments corresponding to the Z19 and Z22 fractions, respectively. The helices are folded upon each other in an antiparallel fashion, linked at each end by glutamine-rich turns or loops, and stabilized by hydrogen bonds. Matsushima et al. (7) proposed that the helices were

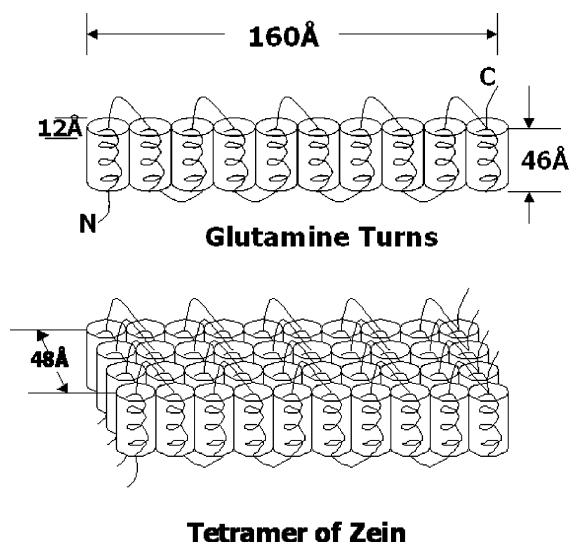
aligned to form a compact prism of 160 Å in length and 46 Å in height for nonreduced zein. The width of the prism was ~12 Å (see **Figure 1**). The structure of zein films plasticized with oleic acid was investigated by small-angle X-ray scattering (SAXS) (8). Films showed a strong periodicity ($d = 135$ Å) across the film plane, suggesting the formation of layers along the plane of the film. A layered structure in zein films could have developed during the resin preparation process and then become aligned during film formation. Oleic acid seemed to play an important role in layer formation. Granular unplasticized zein did not show any SAXS periodicity. Lai et al. (8) proposed a structural model for drawn films based on their X-ray measurements and the zein molecular dimensions determined by Matsushima et al. (7) for nonreduced zein. Layers of double-stacked zein units, measuring 160 Å in length and 2(46 Å) in height, alternated with bilayers of oleic acid (42 Å) to form a structure with a periodicity of ~135 Å.

Interactions between zein and oleic acid in drawn films were investigated by differential scanning calorimetry (DSC) (2). DSC thermograms of zein films showed no melting peaks for oleic acid, suggesting that a strong protein–lipid interaction prevented phase separation and melting out of oleic acid. Similar results were obtained by Wang et al. (9). Parris and co-workers (10) studied the lipid fraction associated with zein extracted from freshly ground corn kernels. They found that 15–20% of lipids

* Author to whom correspondence should be addressed [telephone (217) 333-9336; fax (217) 333-9329; e-mail gwpadua@uiuc.edu].

[†] Department of Food Science and Human Nutrition.

[§] Department of Biochemistry.



Tetramer of Zein

Figure 1. Zein monomer and tetramer structures derived from Matsushima et al. (7).

present in zein isolates were endogenous free fatty acids, indicating the ability of zein for binding free fatty acids. Forato et al. (11) investigated the interaction between zein and fatty acids within protein bodies by NMR spectroscopy. They observed a broad signal around 172 ppm for the carboxyl headgroup and interpreted it as evidence of decreased mobility of the headgroups with respect to the hydrocarbon chain. Data suggested that the interaction between α -zein and fatty acids took place through the headgroups of fatty acids.

In this work, surface plasmon resonance (SPR) was employed to further investigate protein–lipid interactions in zein–oleic acid films. SPR is an optical technology useful to detect refractive index changes at the surface of a sensor chip. Briefly, the SPR technique is based on the resonant excitation of the surface electrons in a thin metallic gold or silver layer by an evanescent field (12) generated by the total reflection of light at the internal surface of a prism that is in optical contact with the metal film. At a certain angle of incidence, namely, the SPR angle, a minimum in the total reflectivity of a polarized light is observed. The angle depends on the dielectric environment of the exposed metal surface, and it will change to higher values when adsorption on the surface occurs. SPR has a very high sensitivity, allowing the detection of refractive index differences in layers thinner than $1/1000$ of a wavelength. For this reason, the phenomenon has been utilized extensively in studies of surfaces and thin films (13, 14). Moreover, SPR has been used to study dynamic interactions of the molecule–ligand–receptor type (15) to examine adsorption of proteins to metal and polymer surfaces (16, 17) and to study compatibility of biomaterials (18). Also, SPR has become a tool for investigating the biochemical and biophysical properties of membrane protein systems (19) because it is capable of monitoring both the binding of protein to the lipid membrane as well as changes in the structure of the lipid or lipoprotein phase. Soulages et al. (20) investigated the effect of diacylglycerol (DG) concentration on the binding of an insect apolipoprotein to a supported phosphatidylcholine (PC) bilayer. They measured protein monolayers 55–110 Å at the PC membrane, depending on DG concentration. The present work explores the potential of SPR as an analytical tool for studying zein adsorption on the surfaces of fixed carboxylic acid- or methyl-terminated self-assembled monolayers (SAMs) in order to further investigate protein–plasticizer interactions occurring in zein films. Surface morphology of adsorbed zein layers was examined by atomic force microscopy (AFM).

MATERIALS AND METHODS

Reagents. Commercial zein, regular grade F4000 (Freeman Industries Inc., Tuckahoe, NY), reportedly contained 14.9% nitrogen, 1.03% ash, and 1.18% crude fat (21). Zein was used without further treatment. Ethyl alcohol, 200 proof, was obtained from AAPER Alcohol, Shelbyville, KY. Isopropyl alcohol, electronic use; chloroacetic acid, certified; sulfuric acid, certified; and hydrogen peroxide 30%, ACS certified, were from Fisher Scientific, Fair Lawn, NJ.

Gel Electrophoresis. Sodium dodecyl sulfate–polyacrylamide gel electrophoresis (SDS–PAGE) of commercial zein was carried out in an SDS–12% polyacrylamide gel (SDS–Polyacrylamide Gel System, Bio-Rad Laboratories, Hercules, CA) with a running buffer containing 49 mM Tris, 384 mM glycine, and 0.1% (w/v) SDS, pH 8.5. Coomassie blue staining was used for detection of polypeptides. Molecular weights of SDS–PAGE standards ranged from 10 to 220 kDa.

SPR Sample Preparation. Zein solutions of 0.00, 0.01, 0.03, 0.05, 0.10, 0.30, 0.50, 0.75, and 1.00% w/v zein were prepared by stirring the proper amount of zein in aqueous ethanol or 2-propanol, both 75% (volume of alcohol/volume of alcohol and water). The pH of aqueous alcohols had been previously adjusted to 3.55–3.85 with chloroacetic acid. SPR substrates were gold-coated glass microscope slides. Before metal evaporation, glass slides (Fisher Scientific) were thoroughly cleaned with a mixture of concentrated sulfuric acid and 30% hydrogen peroxide (2:1 volume ratio) at 60 °C for 1 h. The dried slides were then coated with a 20 Å chromium (Kurt Lesker, Clairton, PA) adhesion layer at 0.2 Å/s and a 490–500 Å gold (99.99% purity) overlayer at 0.5 Å/s by resistive evaporation under a pressure of 4×10^{-6} Torr. Chromium was applied to ensure good adhesion of the gold layer because gold coatings can be easily peeled off from glass.

For the preparation of carboxylic acid-terminated or methyl-terminated SAMs, gold-coated slides were rinsed with ethanol and immersed in a 2 mM ethanolic solution of 11-mercaptopundecanoic acid or 1-octanethiol for a period of several hours to overnight (22, 23). Slides thus prepared were rinsed with a large amount of ethanol and dried with filtered nitrogen. 11-Mercaptopundecanoic acid and 1-octanethiol were chosen for their availability and because they could represent the hydrophilic and hydrophobic endings of oleic acid.

SPR Apparatus. The SPR apparatus used in this experiment was custom-constructed on the basis of the Kretschmann configuration. A beam of light from a 5 mW Ga–As laser ($\lambda = 665$ nm) passed through a triangular prism and was directed to the backside of a gold film deposited onto a microscope slide. Slides were sealed to the equilateral triangle prism (Mellis Griot) using index-matching oil. A flow cell (0.4 mL) was used to measure the equilibrium protein adsorption. A system of three-way valves allowed the changing of solutions without introducing air into the cell. The laser beam passed through two polarizers, which controlled light intensity and produced p-polarized light at the sample. The photodiode, used for detecting the reflected light, was supported on a rotatable bracket mounted concentrically with the prism table, the rotation of both being achieved by computer-controlled rotary stepper motors (Arrick). The resonance condition was determined by recording the reflected light intensity as a function of the angle of incidence. SPR monitors the sample center to avoid edge effects due to capillary forces. The entire apparatus was mounted on an optical bench in a darkroom and routinely checked for alignment before any measurements were taken.

SPR Analysis. After deposition of SAMs, slides were mounted on the SPR cell under water. A zein solution (6–7 mL or 15 SPR cell volumes) was then injected into the cell and allowed to stand to equilibrate for 4 h. The cell was later flushed with distilled water to replace the ethanolic solution before SPR angle changes were measured. Flushing with water was necessary because the SPR instrument used could detect signal changes only under water. The dependence of the reflected beam intensity, I_r , on the incident angle, Θ , was measured for each sample before and after deposition of the overlayers. I_r versus Θ profiles were fitted to theoretical dispersion curves, which were calculated using Fresnel reflectivity coefficients for a multilayer system (24). The procedure was carried out with a commercial program purchased from the Institute of Semiconductor Physics (Kiev, Ukraine). Provided that the refractive index, n , of the sample material in the dry

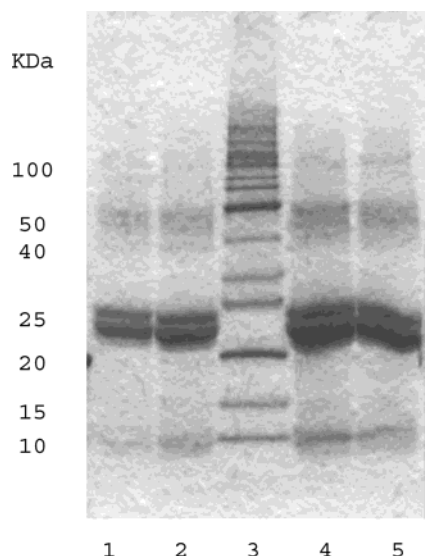


Figure 2. SDS-PAGE of commercial zein: (lanes 1 and 2) 0.25% w/v zein; (lane 3) molecular weight standards; (lanes 4 and 5) 0.5% w/v zein.

state is known, the simulation allows the determination of a calibration slope, k , that relates the changes in the resonance angle, Θ_r , to the changes in the effective optical thickness, d , of the sample layer, $\Delta d = k\Theta_r$. It should be noted that the total thickness of all the layers on the surface of a gold metal film was always <80 nm. At that distance, the instrumental output parameter, Θ_r , varies linearly with the surface density of the material present at the solid-liquid interface (25).

AFM Analysis. AFM, Dimension 3100 (Digital Instruments, CA), was used to examine the surface of SAMs and zein deposits. SPR slides were placed in desiccators after the SPR experiment and allowed to dry for 24 h before AFM scans were taken. AFM measurements were carried out using a Nanoscope IIIa controller. Silicon nitride probes mounted onto cantilevers were used with a scan frequency of 2 Hz.

RESULTS AND DISCUSSION

Molecular Weight Distribution of Commercial Zein.

Figure 2 shows the electrophoretic profile of commercial (Freeman) zein at two different concentrations. Two intense bands were observed between 22 and 24 kDa (for all lanes), confirming that the sample consisted largely of α -zein monomer. A weak band was observed at ~ 47 kDa corresponding to the dimer of α -zein. Results were consistent with previous reports (26, 27) on the molecular weight distribution of commercial zein.

Zein Adsorption to 11-Mercaptoundecanoic Acid Supported by Gold-Coated Slides. The effect of zein concentration (0.01–1.0% w/v) on the SPR reflectivity profile is shown in **Figures 3** and **4** for 2-propanol and ethanol solutions, respectively. The blank, where the SPR angle shift is zero, was 11-mercaptoundecanoic acid deposited on a gold substrate. 11-Mercaptoundecanoic acid formed carboxylic acid-terminated SAMs, which generated a hydrophilic surface exposed to the zein solution in the SPR cell (22). The adsorbed zein layer was then flushed with distilled water so that all deposits were detected under water. **Figures 3** and **4** show SPR angle shifts with increasing zein concentration. Because each angle change profile was measured from a baseline generated by its supporting gold slide, profiles in the two figures were standardized to a common baseline. It is important to emphasize that no major changes occurred in the shape of the resonance curves over the entire zein concentration range. This indicated that there were no large structural alterations occurring in the 11-mercaptoundecanoic acid layer. It was observed that zein solutions of higher

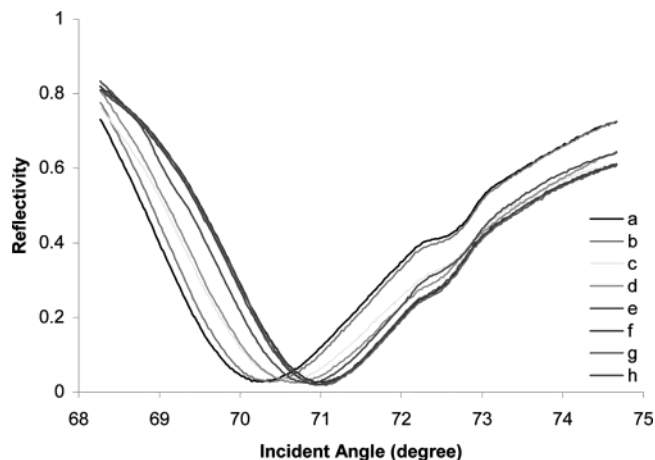


Figure 3. Effect of zein concentration on SPR angle shift: (a) blank; (b) 0.01%; (c) 0.03%; (d) 0.05%; (e) 0.1%; (f) 0.3%; (g) 0.5%; (h) 1.0%. Zein was dissolved in 75% 2-propanol.

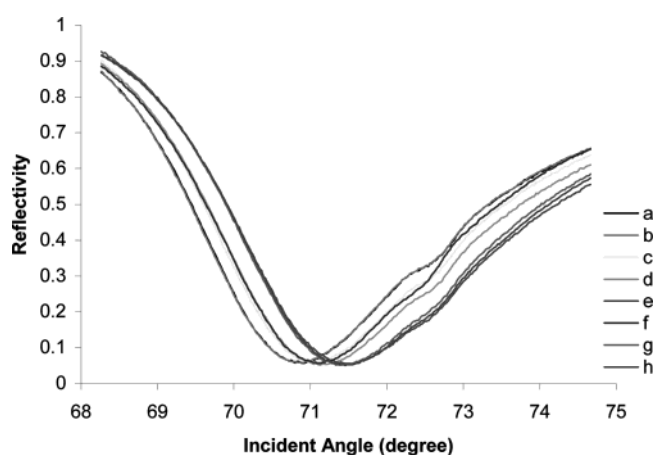


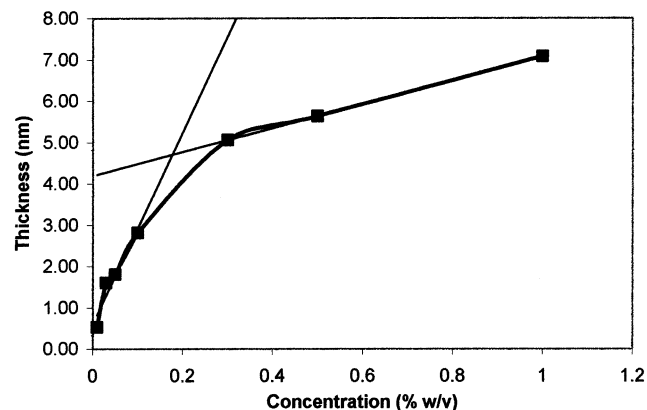
Figure 4. Effect of zein concentration on SPR angle shift: (a) blank; (b) 0.01%; (c) 0.03%; (d) 0.05%; (e) 0.1%; (f) 0.3%; (g) 0.5%; (h) 1.0%. Zein was dissolved in 75% ethanol.

concentration had larger angle shifts, suggesting more protein was bound to the 11-mercaptoundecanoic acid. It was believed that at very low concentrations (0.01% w/v) zein covered the surface only partially, whereas at higher concentrations coverage was more extensive, increasing the angle shift. At concentrations beyond 3.0% w/v, zein solutions became cloudy, suggesting protein aggregation (28). Flushing with water may have enhanced zein to zein interactions due to the polar environment created by water. Therefore, larger angle shifting in this region could be expected not only because of a larger number of protein molecules present but also due to protein aggregation. The interaction between zein and 11-mercaptoundecanoic acid was considered to be of a polar nature because it involved fatty acid carboxylic groups at low pH (3.5–3.8).

SPR angle shifts and derived thickness for zein layers are presented in **Table 1**. ANOVA analysis determined that the difference in thickness for zein depositions in ethanol or 2-propanol was not significant. Therefore, ethanol and 2-propanol data for thickness changes at each concentration level were pooled and are shown in **Figure 5**. The graph was thought to represent two adsorption stages, before surface saturation at 0–0.1% w/v zein and multilayer adsorption from 0.3 to 1.0% w/v. Therefore, a bilinear regression was drawn to detect the surface saturation point. The continuous curve passed through all experimental data. **Figure 5** shows a steep slope for layer thickness at low zein concentrations from 0 to 0.1% w/v

Table 1. Effect of Protein Concentration on SPR Angle and Thickness of Zein Layer Adsorbed to Carboxylic Acid-Terminated (Polar) Surfaces

zein concn (% w/v)	75% ethanol		75% 2-propanol	
	SPR angle (deg)	approx film thickness (nm)	SPR angle (deg)	approx film thickness (nm)
SAM	70.47	0	70.62	0
0.01	70.52 ± 0.04	0.18 ± 0.04	70.77 ± 0.06	0.88 ± 0.18
0.03	70.76 ± 0.08	1.88 ± 0.68	70.82 ± 0.05	1.19 ± 0.29
0.05	70.83 ± 0.11	2.24 ± 0.71	70.82 ± 0.04	1.15 ± 0.27
0.1	71.03 ± 0.02	3.29 ± 0.16	71.01 ± 0.16	2.39 ± 0.96
0.3	71.34 ± 0.29	5.17 ± 1.76	71.44 ± 0.21	4.95 ± 1.27
0.5	71.36 ± 0.27	5.15 ± 1.96	71.54 ± 0.24	5.68 ± 1.47
1.0	71.65 ± 0.49	7.22 ± 2.00	71.76 ± 0.38	6.96 ± 2.40

**Figure 5.** Thickness change of zein layers deposited on 11-mercaptoundecanoic acid surfaces.

(slope = 23.2, $R^2 = 0.9231$). The slope decreased from 0.1 to 1.0% w/v zein w/v (slope = 2.9, $R^2 = 1$). The intercept of these two lines was interpreted as the surface saturation point. Zein was considered to form a monolayer, 4.7 nm in thickness, on 11-mercaptoundecanoic acid surfaces.

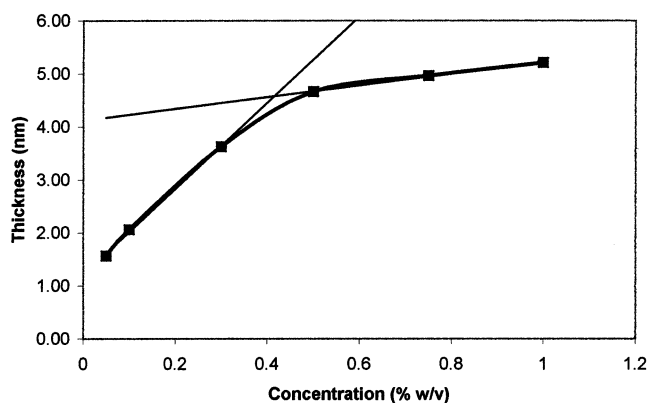
In previous studies, Lai et al. (8) proposed a platelet structural model for drawn films based on X-ray measurements. They reported a spacing of 135 Å corresponding to double layers of oleic acid and a double stack of zein. Their model suggested that the basic zein structural units were composed of ribbons of folded (antiparallel) α -helical segments with a fold period of ~ 4.6 nm including the folds. The interaction between zein and oleic acid was thought to be through H-bonding between the carboxyl heads of the fatty acid and the glutamine residues at the zein surface (see **Figure 1**). The SPR experiment detected a layer of zein, 4.7 nm in thickness, adsorbed to the carboxyl heads of 11-mercaptoundecanoic acid. This measurement is very close to the proposed height of zein units in the model by Lai et al. (8) for the structure of zein-oleate films. Zein aggregates beyond this layer were not easily characterized by SPR.

Zein Adsorption to 1-Octanethiol Supported by Gold-Coated Slides. The adsorption of zein onto hydrophobic surfaces was also investigated by SPR. Gold-coated slides were immersed in the 2 mM 1-octanethiol solution to allow the self-assembly of a monolayer and the generation of a hydrophobic surface. The methyl-terminated surfaces are low-energy surfaces and are therefore less prone to contamination (29).

Zein concentration, SPR angle shift, and surface thickness are listed in **Table 2**. **Figure 6** shows the growth of zein deposits on a nonpolar surface. The trend was similar to that of zein deposited on polar surfaces, as described above. At low zein concentrations (0.01–0.3% w/v) the rate of increase for zein thickness had a slope of 8.1. Above 0.3% w/v the slope

Table 2. Effect of Protein Concentration on SPR Angle and Thickness of Zein Layer Adsorbed to Methyl-Terminated (Nonpolar) Surfaces

zein concn (% w/v)	75% 2-propanol	
	SPR angle (deg)	approx film thickness (nm)
SAM	70.54	0
0.05	70.79 ± 0.01	1.57 ± 0.10
0.1	70.87 ± 0.04	2.06 ± 0.23
0.3	71.12 ± 0.01	3.63 ± 0.15
0.5	71.29 ± 0.01	4.72 ± 0.08
0.75	71.34 ± 0.26	4.96 ± 1.56
1.0	71.37 ± 0.31	5.21 ± 1.93

**Figure 6.** Thickness change of zein layers deposited on 1-octanethiol surfaces.

decreased to 1.1, indicating equilibrium was established, and a fixed layer of 4.6 nm was formed.

Matsushima et al. (7) proposed, from X-ray measurements on zein secondary structure, that zein molecules have a prism-shaped structure with surfaces of different polarities. The two opposite surfaces that are rich in glutamine turns or loops were considered to be polar. The other two pairs of surfaces parallel to the α -helix were thought to be nonpolar. Binding of zein on methyl-ended surfaces as detected by SPR was considered to be a hydrophobic interaction between the nonpolar surfaces of the zein prism and methyl groups at the surface of the SPR cell. Moreover, the step of washing the surface with water creates a polar environment and promotes the hydrophobic interaction of zein to zein aggregates. The measured layer of zein (~ 4.6 nm) is close to that of a zein tetramer (4.8 nm, see **Figure 1**) (7).

Although proteins have been observed to spread and reorient upon adsorption to various surfaces, no spreading or conformational changes were detected in this experiment. The estimated thickness of the zein monolayer on 11-mercaptoundecanoic acid corresponds to the height of the zein molecule according to Matsushima et al. (7). The consistency of those values suggested that zein maintained the prism shape after adsorption.

AFM Surface Characterization of Zein Deposits. The surface topography of zein deposits over SAMs of carboxylic acid-terminated thiol [$\text{COOH}(\text{CH}_2)_{10}\text{SH}$] or methyl-terminated alkanethiol [$\text{CH}_3(\text{CH}_2)_7\text{SH}$] on gold-coated SPR slides was investigated by AFM. Images of SAMs were also obtained. All images were taken within the center of the SPR flow channel, to avoid regions of abnormal adsorption at the sides of channels. **Figures 7 and 8** correspond to surface plots of the hydrophilic and hydrophobic SAMs. The hydrophilic surface appears to be uniformly smooth, with a grain diameter ranging from 59 to 64

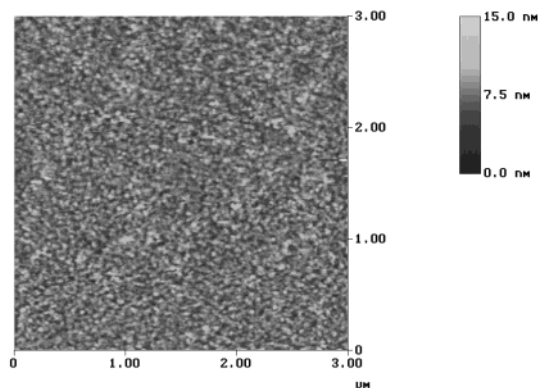


Figure 7. AFM image of SAMs of 11-mercaptoundecanoic acid on a gold surface.

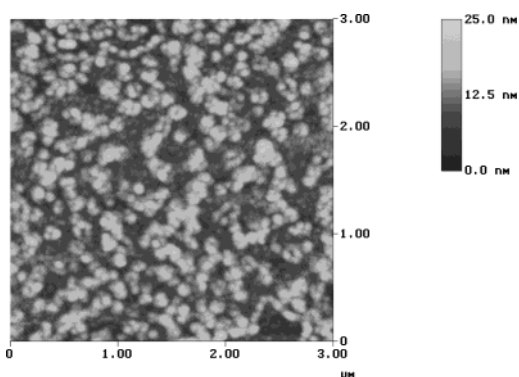


Figure 8. AFM image of SAMs of 1-octanethiol on a gold surface.

nm. The hydrophobic surface is rougher, with the grain diameter ranging from 94 to 117 nm. Roughness was calculated using root-mean-square (rms) deviation of the heights of the various features imaged by AFM (29) as

$$\text{rms} = [(Z_1^2 + Z_2^2 + Z_3^2 + \dots + Z_N^2)/N]^{0.5}$$

where Z_i are the height deviations from the data plane. It shows maximum height variations of 11–15 nm for hydrophilic surfaces (rms = 1.27 nm) and 20–24 nm for hydrophobic surfaces (rms = 3.41 nm), both indicating high surface coverage for these compounds.

AFM images of zein adsorbed to hydrophilic and hydrophobic surfaces are shown in **Figures 9** and **10**. They both show surface topography changes with respect to their corresponding SAMs. Roughness, calculated as above, for zein on hydrophilic surfaces was ~5.30 nm, which is 4 times larger than its base SAM. However, on hydrophobic surfaces roughness decreased from 3.41 to 1.81 nm after zein adsorption. From a comparison of the two images, it was observed that they have different surface features. Zein adsorbed to hydrophilic surfaces (**Figure 9**) showed the development of ring-shaped structures of average height of 45 nm, which is 5 times higher than the base surface. A possible explanation on how zein cylinders were formed is that zein was first bound to the carboxylic head of 11-mercaptoundecanoic acid to form wormlike strings and circles, which provided the base structure. Then, excess zein molecules attached themselves to the circular base, piling up to form a high tube. During this process, the environment polarity is critical. Initially, zein was dissolved in 75% alcohol, which because of its relatively low polarity promoted zein to carboxylic head interactions. Later on, when the SPR cell was flushed with water, the polarity of the solution increased sharply, promoting zein aggregation through hydrophobic interactions.

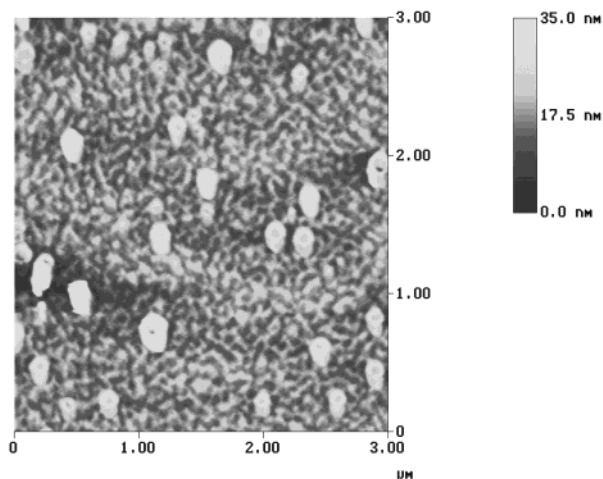


Figure 9. AFM image of zein adsorbed to 11-mercaptoundecanoic acid surfaces.

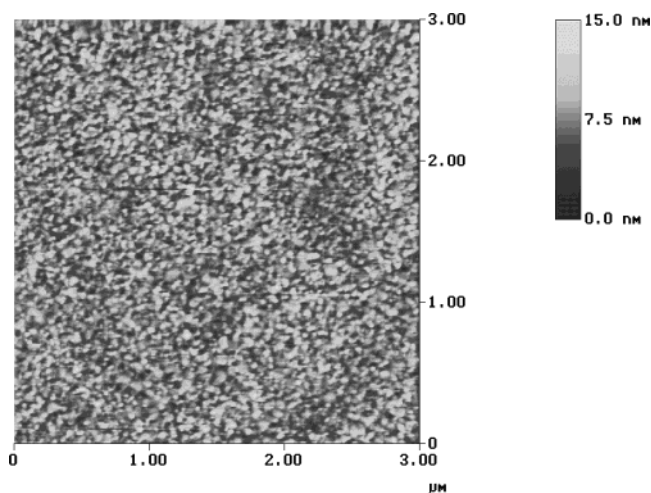


Figure 10. AFM image of zein adsorbed onto 1-octanethiol surfaces.

In contrast, the topography of zein adsorbed to hydrophobic surfaces was more uniform (**Figure 10**) than the one described above. Because in this experiment the alkanethiol surface is formed by methyl groups, only the nonpolar surfaces of zein would have affinity for and interact with them. A uniform coverage indicated that zein molecules adsorbed to the methyl-terminated SAM surface in a homogeneous way, showing low surface height and no salient structural features. Because zein has hydrophilic and hydrophobic surfaces, it formed different structures if deposited on polar or nonpolar surfaces, influenced by the environment polarity. AFM results served to identify different surface structures formed by zein adsorbed onto hydrophilic or hydrophobic surfaces. Clearly these will require more extensive investigation. Those studies are in progress and will be reported in detail elsewhere.

ACKNOWLEDGMENT

We thank Tim Miller and Todd Holland for their help in building and setting up the SPR instrument.

LITERATURE CITED

- (1) Gennadios, A.; Weller, C. L. Edible films and coatings from wheat and corn proteins. *Food Technol.* **1990**, *44*, 63–69.
- (2) Lai, H.-M.; Padua, G. W. Properties and microstructure of plasticized zein films. *Cereal Chem.* **1997**, *74*, 771–775.

- (3) Reiners, R. A.; Wall, J. S.; Inglett, G. E. Corn proteins: potential for their industrial use. In *Industrial Uses of Cereals*; Pomeranz, Y., Ed.; Symposium Proceedings of the 58th Annual Meeting of the AACCC; AACCC: St. Paul, MN, 1973; pp 285–302.
- (4) Santosa, F. X. B.; Padua, G. W. Tensile properties and water absorption of zein sheets plasticized with oleic and linoleic acids. *J. Agric. Food Chem.* **1999**, *47*, 2070–2074.
- (5) Santosa, F. X. B.; Padua, G. W. Thermal behavior of zein sheets plasticized with oleic acid. *Cereal Chem.* **2000**, *77*, 459–462.
- (6) Argos, P.; Pederson, K.; Marks, M. D.; Larkins, B. A. Structure model for maize zein proteins. *J. Biol. Chem.* **1982**, *257*, 9984–9990.
- (7) Matsushima, N.; Danno, G. I.; Takezawa, H.; Izumi, Y. Three-dimensional structure of maize α -zein proteins studied by small-angle X-ray scattering. *Biochim. Biophys. Acta* **1997**, *1339*, 14–22.
- (8) Lai, H.-M.; Geil, P. H.; Padua, G. W. X-ray diffraction characterization of the structure of zein-oleic acid films. *J. Appl. Polym. Sci.* **1999**, *71*, 1267–1281.
- (9) Wang, Y.; Rakotonirainy, A. M.; Padua, G. W. Thermal behavior of zein-based biodegradable films. *Starch/Staerke* **2003**, *55*, 25–29.
- (10) Parris, N.; Dickey, L. C.; Powell, M. J.; Coffin, D. R.; Moreau, R. A.; Craig, J. C. Effect of endogenous triacylglycerol hydrolysates on the mechanical properties of zein films from ground corn. *J. Agric. Food Chem.* **2002**, *50*, 3306–3308.
- (11) Forato, L. A.; Colnago, L. A.; Garratt, R. C.; Lopes, M. A. Identification of free fatty acids in maize protein bodies and purified α zeins by ^{13}C and ^1H nuclear magnetic resonance. *Biochim. Biophys. Acta* **2000**, *1543*, 106–144.
- (12) Knoll, W. Interfaces and thin films as seen by bound electron-magnetic waves. *Annu. Rev. Phys. Chem.* **1998**, *49*, 569–638.
- (13) Abeles, F.; Lopez-Rios, T.; Tadjeddine, A. Investigation of the metal–electrolyte interface using surface plasma waves with ellipsometric detection. *Solid State Commun.* **1975**, *16*, 843–847.
- (14) Rothenhäuser, B.; Cuschl, C.; Knoll, W. Plasmon surface polariton fields for the characterization of thin films. *Thin Solid Films* **1988**, *159*, 323–330.
- (15) Bondeson, K.; Frostell-Karlsson, A.; Fagerstam, L.; Magnusson, G. Lactose repressor-operator DNA interactions: kinetic analysis by a surface plasmon resonance biosensor. *Anal. Biochem.* **1993**, *214*, 245–251.
- (16) Delden, C. J. V.; Lens, J. P. L.; Kooyman, R. P. H.; Engbers, G. H. M. Heparinization of gas plasma-modified polystyrene surfaces and the interactions of these surfaces with proteins studied with surface plasmon resonance. *Biomaterials* **1997**, *18*, 845–852.
- (17) Green, R. J.; Davies, J.; Davies, M. C.; Roberts, C. J.; Tendler, S. J. B. Surface plasmon resonance for real time in situ analysis of protein adsorption to polymer surfaces. *Biomaterials* **1997**, *18*, 405–413.
- (18) Davies, J.; Allen, A.; Bruce, I. Dynamic, in-situ, techniques for probing surface properties of biomaterials. In *Proceedings of the International Conference of Surface Properties of Biomaterials*; Butterworth-Heinemann: Cambridge, U.K., 1994; pp 117–132.
- (19) Salamon, Z.; Tollin, G. Surface plasmon resonance studies of complex formation between cytochrome *c* and bovine cytochrome *c* oxidase incorporated into a supported planar lipid bilayer. I. Binding of cytochrome *c* to cardiolipin/phosphatidylcholine membranes in the absence of oxidase. *Biophys. J.* **1996**, *71*, 848–857.
- (20) Soulages, J. L.; Salamon, Z.; Wells, M.; Tollin, G. Low concentration of diacylglycerol promote the binding of apolipoprotein III to a phospholipid bilayer—A surface plasmon resonance spectroscopy study. *Proc. Natl. Acad. Sci. U.S.A.* **1995**, *92*, 5650–5654.
- (21) Fu, D. Zein Properties and Alternative Recovery Methods. Ph.D. Dissertation, Department of Food Science and Technology, University of Nebraska at Lincoln, 1999.
- (22) Bain, C. D.; Troughton, E. B.; Tao, Y. T.; Evall, J.; Whitesides, G. M.; Nuzzo, R. G. Formation of monolayer films by the spontaneous assembly of organic thiols from solution onto gold. *J. Am. Chem. Soc.* **1989**, *111*, 321–335.
- (23) DeBono, R. F.; Loucks, G. D.; Manna, D. D.; Krull, U. J. Self-assembly of short and long-chain *n*-alkane thiols onto gold surfaces: A real-time study using surface plasmon resonance techniques. *Can. J. Chem.* **1996**, *74*, 677–688.
- (24) Drake, P. S. Surface-enhanced Raman and Surface Plasmon Resonance Measurements of Case II Diffusion Events on the Nanometer Length Scale. Ph.D. Dissertation, Department of Analytical Chemistry, University of Illinois at Urbana–Champaign, 1995.
- (25) Jung, L. S.; Campbell, C. T.; Chinowsky, T. M.; Mar, M. N.; Yee, S. S. Quantitative interpretation of the response of surface plasmon resonance sensors to adsorbed films. *Langmuir* **1998**, *14*, 5636–5648.
- (26) Wilson, C. M. Electrophoretic analyses of various commercial and laboratory-prepared zeins. *Cereal Chem.* **1988**, *65*, 72–73.
- (27) Wang, J.; Geil, P. H.; Padua, G. W. Analysis of zein by matrix-assisted laser desorption/ionization mass spectrometry. *J. Agric. Food Chem.* **2003**, *51*, 5849–5854.
- (28) Augustine, M. E.; Baianu, I. C. Basic studies of corn proteins for improved solubility and future utilization: a physicochemical approach. *J. Food Sci.* **1987**, *52*, 649–652.
- (29) Huang, Y.-W.; Gupta, V. K. Effects of physical heterogeneity on the adsorption of poly(ethylene oxide) at a solid–liquid interface. *Macromolecules* **2001**, *34*, 3757–3764.

Received for review January 22, 2003. Revised manuscript received September 2, 2003. Accepted September 18, 2003. This research was supported in part by the Illinois Corn Marketing Board. We appreciated the help from the Center for Microanalysis of Materials, University of Illinois, which is partially supported by the U.S. Department of Energy under Grant DEFG02-91-ER45439.

JF0340658